

## AN OBSERVATION OF COSMIC RAY POSITRONS FROM 10-20 GEV\*

Dietrich Müller<sup>†</sup> and Jonathan Tang  
 Enrico Fermi Institute, University of Chicago  
 Illinois 60637 USA.

**ABSTRACT** A balloon flight of the University of Chicago electron telescope has been performed in Hawaii in April 1984. Making use of the east-west asymmetry in the geomagnetic cut-off rigidity, we have successfully separated the cosmic-ray positrons and negatrons over the range 10-20 GeV. The positron to electron ratio,  $e^+/(e^++e^-)$ , was measured to be  $17\pm 5\%$ , significantly higher than the ratio measured in the 1-10 GeV range by other experiments. This increase appears to suggest that either a primary component of positrons become significant above 10 GeV, or that the spectrum of primary negatrons decreases above 10 GeV more sharply than that of secondary positrons.

**INTRODUCTION** Cosmic ray electrons consist of both positrons and negatrons. Present measurements of the combined positron and negatron flux cover energies up to almost 1000 GeV, while data on the charge composition beyond 10 GeV are very scarce. The combined energy spectrum exhibits a characteristic steepening around 30 GeV, which is commonly attributed to radiative energy losses in interstellar space. If interpreted in the context of the leaky box model, the steepening is consistent with a galactic containment time of  $10^7$  years, in close agreement with results based on measurements of the  $^{10}\text{Be}$  abundance. However, these interpretations of the electron spectrum are usually made under the assumption that the source spectrum of electrons follows that of nuclear cosmic rays and that the electron flux is dominated by primary negatrons. This assumption must be verified by separate measurements of positrons and negatrons: Both positrons and negatrons are produced in about equal proportions as secondary products of interactions of cosmic ray nuclei with interstellar gas. The source spectrum of these secondary particles is directly related to the spectrum of parent particles (mostly protons) and can be calculated with good accuracy for various propagation models (Orth & Buffington, 1976). Any significant excess of negatrons, however, must be attributed to primary acceleration in cosmic ray sources. Below 10 GeV, such primary negatrons have been found to be the dominant component.

Most of the existing data on cosmic ray positrons come from balloon borne magnet spectrometers (Fanselow et al 1969, Buffington et al 1975, Daugherty et al 1975), but both momentum resolution and counting statistics have limited the accessible energy range. An alternate opportunity to separate positive and negative particles is provided by the earth's magnetic field. The cut-off rigidity varies with the geographic location, the direction of incidence of the particle and with the particle charge. The cut-off rigidities for negatrons at Hawaii are shown in figure 1.

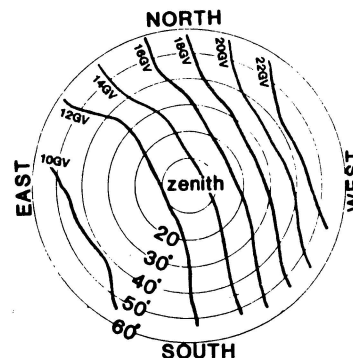


Fig.1 View of Sky, Hawaii  
 contours of negatron cutoff rigidities

\* Supported, in part, by NASA grant NSG-7464.

<sup>†</sup> Also Department of Physics.

For positrons, east and west exchange roles. Therefore, there exists a range of energies and directions for which, for a given geographic location, the earth's field transmits only particles of one polarity. The utilization of this effect was pioneered by Daniel and Stephens (1965,1967). However, the first measurements (Anand et al, 1969; Agrinier et al, 1969) were severely limited due to insufficient statistics and systematic uncertainties.

In April 1984, we have performed a balloon flight from Hawaii using our electron telescope to separate negatrons and positrons in the range 10-20 GeV. The flight had a duration of 11 hours at a float altitude corresponding to  $4 \text{ gm/cm}^2$  residual atmosphere in the vertical. The following describes our measurement.

INSTRUMENTATION This instrument has been described previously in detail (Tang, 1984). Here we just summarize the main features: The instrument is an electronic counter telescope with a geometric factor of about  $0.1 \text{ m}^2$  sterad. For each particle traversing the detector, the following quantities are measured: (1) the charge number  $|z|$  with a plastic scintillator, (2) the trajectory through the instrument with a multiwire proportional chamber hodoscope, (3) the direction of traversal with a time-of-flight measurement, (4) the transition radiation emitted by electrons (but not protons) in a 6-layer transition radiation detector, and (5) the electromagnetic cascades produced in a 9 layer lead-scintillator shower detector of 18.5 radiation length depth. These cascades are characteristic for electrons and measure the electron energy with  $\Delta E/E \approx 8\%$ .

During the balloon flight, the instrument has been suspended with its axis inclined by 30 degrees against the vertical. The orientation of the gondola was measured with magnetometers, and, through the use of a commandable torque motor, the instrument could be oriented towards the west (to observe positrons) or towards the east (for a control measurement of negatrons). To determine the cut-off rigidities (shown in fig.1), we use the predictions of Shea and Smart (1974), and we note that cosmic ray measurements of Jordan and Meyer (1983) have been in agreement with these predictions.

ANALYSIS & RESULTS Electrons are selected from the data set according to procedures described in detail in our earlier work (Tang, 1984). Due to the combination of a deep shower detector with a transition radiation detector, our instrument is capable of rejecting protons with the required rejection power of  $10^4$ . The residual proton contamination to our results is indicated in table 1. After applying the appropriate corrections for inefficiencies of individual detector elements, for the area-exposure time, and for energy losses in the residual atmosphere above the detector, we obtain the electron fluxes, grouped according to directions of incidence from EAST, and from WEST.

The measured EAST and WEST electron spectra are shown in Figure 2. They exhibit a clear east/west asymmetry between 10 to 20 GeV while showing the same flux at other energies. Cutoffs at 11 GeV (east) and 22 GeV (west) agree well with negatron cut-off calculations, which use codes by

Shea and Smart (1974). Each spectrum can be analyzed as a composite of (i) atmospheric secondary electrons, (ii) secondary electrons that appear as reentrant albedo particles, (iii) galactic negatrons, and (iv) galactic positrons.

Such an analysis for the WEST data is shown in Figure 2. The curve for atmospheric secondaries is derived from interpolating calculations by Beuermann (1971) for 7 gm/cm<sup>2</sup> of atmosphere. The reentrant albedo particles are expected to disappear above cut-off rigidities. In Figure 2, we estimated their fluxes such that the direct atmospheric and the reentrant secondaries add up to our data below 10 GeV. This procedure is consistent with the flux of reentrant albedo electrons at 4 GeV measured by Daniel and Stephens (1967).

The curve of galactic negatrons is obtained by folding our previously measured electron spectrum with calculations of geomagnetic cutoffs. Clearly, a significant amount of positrons is required to account for the fluxes from 10 to 20 GeV.

To derive the positive fraction of cosmic ray electrons, the WEST data are divided into 2 energy intervals shown in Table 1. N(total) is the number of selected events and N(proton) is the estimated number of residual proton background. N(atmos) is the number of atmospheric and reentrant albedo events estimated by extrapolating data below 10 GeV to higher energies. The net number of positrons, N(+), is obtained by subtracting N(proton) and N(atmos) from N(total). We obtain N(sum), the sum of cosmic positrons and negatrons, using the EAST data and our previous measurement (Tang 1984). Finally, a factor f corrects for small effects due to the finite energy resolution of the detector and the variation of cut-off rigidities over extended regions of the sky. The positive fraction,  $e^+/(e^++e^-)$ , is then the ratio of N(+), multiplied by f.

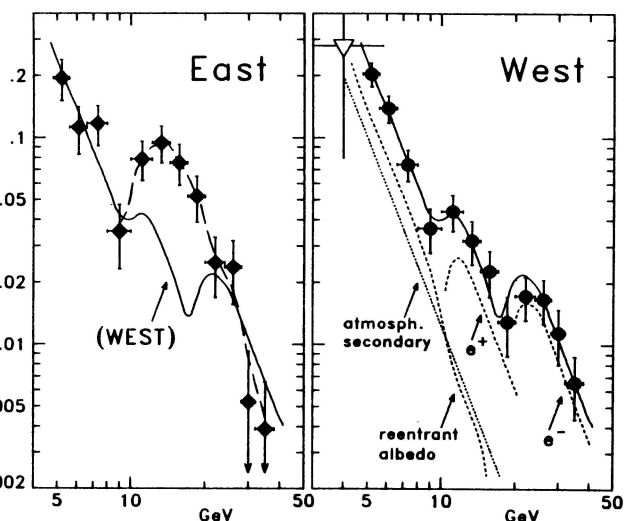


Fig.2 Differential Energy Spectra of Electrons, Hawaii '84  
The solid curve (WEST) is the sum of the dotted curves.  
The dashed curve is a hand fit to the EAST spectrum.  
Reentrant albedo data point:  $\nabla$  Daniel & Stephens '67

E(GeV)	N(total)	N(proton)	N(atmos)	N(+)	N(sum)	f	$e^+/(e^++e^-)$
10-14.4	67 $\pm$ 8.2	9.3 $\pm$ 2.3	22. $\pm$ 5.8	35.8 $\pm$ 10	248 $\pm$ 30	1.05 $\pm$ .05	.151 $\pm$ .048
14.4-20	34 $\pm$ 5.8	3.3 $\pm$ 0.8	8.6 $\pm$ 3.4	22.1 $\pm$ 7.	97 $\pm$ 13	0.90 $\pm$ .10	.204 $\pm$ .072

**DISCUSSION** Our measurements of  $e^+/(e^++e^-)$  in cosmic-ray are shown in Figure 3. The error limits include statistical and systematic uncertainties. We compare our data with measurements at lower energies and with some calculations of propagation models using pathlengths which agree with B/C ratios (Protheroe, 1982). The calculations have shown that

the positron flux below 10 GeV is consistent with an entirely (>97%) secondary origin, due to interactions of nuclei (mostly protons) in the interstellar gas. Our results show an increase of the positive fraction above 10 GeV and are significantly higher than the model calculations.

There are two possibilities to understand this increase of  $e^+/(e^++e^-)$ : (1) a primary component of positrons becomes significant above 10 GeV; or (2) the flux of primary electrons (assumed to be almost entirely negatrons) decreases above 10 GeV more rapidly than that of secondary positrons. The first possibility may not be very likely, while the latter is corroborated by the fact that the total electron spectrum begins to bend over at the same energy region where  $e^+/(e^++e^-)$  increases. Such a decrease of primary negatrons above 10 GeV could, for instance, have its origin in the acceleration region if synchrotron losses in that region limit the electron energies attainable during the acceleration time. Or it may be that sources of primary electrons are significantly further away than those of secondary positrons, leading to comparatively larger energy losses en route.

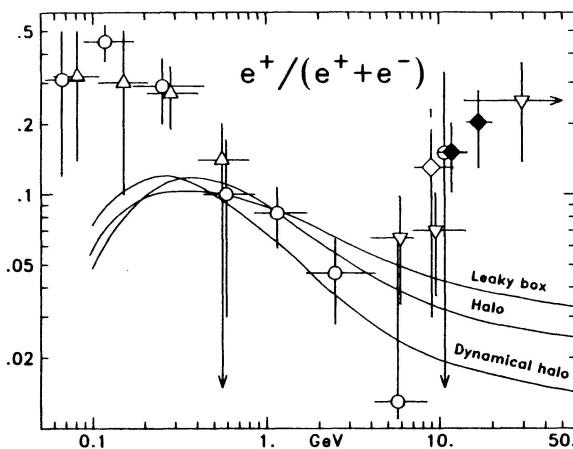


Fig.3 Positive Fraction of Cosmic Ray Electrons  
data:  $\blacklozenge$  This Work,  $\nabla$  Buffington '75,  $\triangle$  Daugherty '75,  
 $\circ$  Fanselow '69,  $\diamond$  Agrinier '69. curves: Protheroe '82.

#### ACKNOWLEDGEMENT

We acknowledge the assistance of E. Drag and the substantial contributions of R. Kroeger towards the success of this experiment, and we are indebted to the crew of the National Scientific Balloon Facility and the U.S. Navy for excellent balloon flight and support operations. We are also grateful for the help of Dr. Peter Meyer in sharing transportation and accommodation of our equipment.

#### References

- Agrinier, et al. *Lettere al Nuovo Cimento, serie I*, 1 53 (1968).  
 Anand, K.C., Daniel R.R., and Stephens S.A., 11th ICRC Budapest (1969).  
 Beuerman, K.P., *J.G.R.*, vol 76, no 19, 4291 (1971).  
 Buffington A., Orth C.D. and Smoot G.F., *Ap. J.* 199 699 (1975).  
 Daniel R.R., and Stephens S.A., *Phys. Rev. Lett.*, 15 769 (1965).  
 Daniel R.R., and Stephens S.A., *Proc. Indian Acad. Sci.*, 65A 319 (1967).  
 Daugherty, J.K., Hartman, R.C. and Schmidt P.J., *Ap. J.*, 198 493 (1975).  
 Fanselow, J.L., Hartman, R.C. Hildebrand, R.H. and Meyer, P., *Ap.J.* 158 771 (1969).  
 Jordan, S. and Meyer, P., 18th ICRC, OG 45 (1983).  
 Orth, C. D. and Buffington, A. , *Ap. J.* 206 312 (1976).  
 Protheroe, R. J., *Ap. J.* 254 391 (1982).  
 Shea, M.A. and Smart, D. F., Tech. Rep. AFCRL-TR-74-0159, Air Force Cambridge Research Lab., Bedford, Ma. (1974).  
 Tang, K., *Ap. J.* 278 881 (1984).